

Please cite as: Jacob, M., Frankl, A., Mitiku Haile, Zwertvaegher, A., Nyssen, J., 2013. Assessing spatio-temporal rainfall variability in a tropical mountain area (Ethiopia) using NOAA's rainfall estimates. International Journal of Remote Sensing, 34:23, 8305-8321. DOI: 10.1080/01431161.2013.837230

Assessing spatio-temporal rainfall variability in a tropical mountain area (Ethiopia) using NOAAs Rainfall Estimates

MIRO JACOB*†, AMAURY FRANKL†, MITIKU HAILE‡, ANN
ZWERTVAEGHER§ and JAN NYSSSEN†

†Department of Geography, Ghent University, Krijgslaan 281 (S8), B-9000 Ghent,
Belgium.

‡Department of Land Resources Management and Environmental Protection, Mekelle
University, P.O. Box 231, Mekelle, Ethiopia.

§Department of Geology, Ghent University, Krijgslaan 281 (S8), B-9000 Ghent,
Belgium.

Abstract

Seasonal and interannual variation in rainfall can cause massive economic loss for farmers and pastoralists, not only because of deficient total rainfall amounts but also because of long dry spells within the rain season. The semi-arid to subhumid mountain climate of the North Ethiopian Highlands is especially vulnerable to rainfall anomalies. In this paper spatio-temporal rainfall patterns are analysed on a regional scale in the North Ethiopian Highlands using satellite-derived Rainfall Estimates (RFE). To counter the weak correlation in the dry season, only the rain season rainfall from March till September is used, responsible for *ca.* 91% of the annual rainfall. Validation analysis demonstrates that the RFEs are well correlated with the Meteorological Station (MS) rainfall data, i.e. 85% for RFE 1.0 (1996-2000) and 80% for RFE 2.0 (2001-2006). However discrepancies indicate that RFEs generally underestimate MS rainfall and the scatter around the trendlines indicates that the estimation by RFEs can be in gross error. A local calibration of RFE with rain gauge information is validated as a technique to improve the RFEs for a regional mountainous study area. Slope gradient, slope aspect and elevation have no added value for the calibration of the RFEs. The estimation of monthly rainfall using this calibration model improved on average by 8%. Based upon

**Corresponding author. Email address: miro.jacob@ugent.be*

the calibration model, annual rainfall maps and an average isohyet map for the period 1996-2006 were constructed. The maps show a general northeast-southwest gradient of increasing rainfall in the study area and a sharp east-west gradient in its northern part. Slope gradient, slope aspect, elevation, easting and northing were evaluated as explanatory factors for the spatial variability of annual rainfall in a stepwise multiple regression with the calibrated average of RFE 1.0 as dependent variable. Easting and northing are the only significant contributing variables (R^2 : 0.86), of which easting has proven to be the most important factor (R^2 : 0.72). The scatter around the individual trendlines of easting and northing corresponds to an increase of rainfall variability in the drier regions. The improved estimation of spatio-temporal rainfall variability in a mountainous region by RFEs is, although the remaining underestimation of rainfall in the southern part of the study area, valuable as input to a wide range of scientific models.

1. Introduction

In drought years, millions of Ethiopians are dependent on assistance (Segele and Lamb 2005), not only because of deficient total rainfall amounts but also because of long dry spells within the rain season (Seleshi and Camberlin 2005). The northern Tigray region is the driest region in the semi-arid to subhumid mountain climate zone of the North Ethiopian Highlands (Nyssen *et al.* 2005). Seasonal and inter-annual variation in rainfall can cause massive economic loss for abundant poor rural farmers (dependent on rain-fed agriculture) and pastoralists (Shanko and Camberlin 1998). The severe impact of successive dry years has been demonstrated repeatedly in Ethiopia, e.g. the droughts of 1973-1974 and 1982-1985 claiming the lives of several hundred thousands of people (Tilahun 2006b). Rainfall is not only of key importance for agriculture (Frankl *et al.* 2013), but also affects land-use and land-cover dynamics (De Mûelenaere *et al.* 2012) and is a driving force of water erosion processes (Frankl *et al.* 2011, Frankl *et al.* 2012). Nevertheless climatological studies have been neglected for a long time in the arid and semi-arid tropical regions (Tilahun 2006a). Recently characterization and variability of rainfall in Ethiopia are more widely studied (Conway 2000, Seleshi and Zanke 2004,

Nyssen *et al.* 2005, Segele and Lamb 2005, Seleshi and Camberlin 2005, Tilahun 2006b, Tilahun 2006a, Cheung *et al.* 2008).

The aim of this paper is to analyse rainfall patterns not only in time, but also spatially for the period 1996-2006. Analysing spatiotemporal rainfall patterns is rendered possible by use of satellite-derived Rainfall Estimates (RFE) and through the establishment of a relation between rainfall measured in Meteorological Stations (MS) and RFE. The advantage of this method is that “satellite rainfall estimates fill in gaps in station observations” (Verdin *et al.* 2005). Besides NOAA-CPC RFE, there are other satellite rainfall products with a high spatial and temporal resolution such as ARC, 1DD, 3B42, CMORPH, TAMSAT. Dinku *et al.* (2007) validated these algorithms for the complex topography of Ethiopia and concluded that CMORPH and TAMSAT performed the best. Nevertheless RFEs are used in this regional study, because of the particularly high spatial resolution (0.1°) and the opportunity to use historical data starting from 1996. The choice for the RFE algorithm is also important given the widespread use within the Famine Early Warning System (FEWS) of USAID, as a tool for climate monitoring over Africa (FEWS NET 2010a). Shrestha *et al.* (2008) have used RFEs to develop a hydrological modelling system of the Bagmati River Basin of Nepal. Senay and Verdin (2003) used the RFE derived Water Requirements Satisfaction Index (WRSI) to calculate seasonal crop water balances.

The validation of RFE in Africa is insufficient and mainly occurred in the west and south of the continent (Dinku *et al.* 2007). Dinku *et al.* (2007) therefore made a validation study over the east African complex topography which indicates that the estimations by RFE 2.0 version performs less well than the RFE 1.0 version. Subsequently, Dinku *et al.* (2010) investigated the effect of mountainous and arid climates on RFEs in East Africa. The RFEs exhibit a moderate underestimation of rainfall over mountainous regions and high overestimation of rainfall over dry regions (Dinku *et al.* 2010).

In this paper the possibilities of using RFEs for spatio-temporal rainfall analysis on a regional scale in a mountainous area is studied. Therefore the RFEs are validated and calibrated for the regional study area using MS rainfall data.

1.1 Climatic background

The North Ethiopian Highlands are part of the ‘African drylands’ characterised by unreliable seasonal rainfall. Rainfall averages (1996-2006) based upon rainfall data of the meteorological stations (without missing values) indicate that rainfall distribution in the study area follows a bimodal rainfall pattern with an unreliable short rainy season preceding the main rain season (figure 1). Rainfall in the North Ethiopian Highlands is the result of two main processes: the dominant process is convective rainfall and orographic rainfall occurs where winds pass topographic obstacles (Daniel 1977). The mean annual rainfall in the Tigray region varies around 600 mm year⁻¹ (Krauer 1988). The daily rain pattern is dominated by afternoon rains (with 47% from 12 to 18 PM) provoked locally by the convective nature of the rains after morning heating of the earth surface (Krauer 1988).

Rainfall in the North Ethiopian Highlands is mainly dependent on the movement of the Intertropical Convergence Zone (ITCZ) (Goebel and Odenyo 1984). The ITCZ is situated south of the equator in Eastern Africa during the winter in the northern hemisphere. The climate of North Ethiopia is then dominated by high pressure cells of the eastern Sahara and Arabia. North-east winds are prominent with dry airstreams from the Sahara that result in dry weather, this period is known as the *bega* season (figure 1) (Westphal 1975, Seleshi and Zanke 2004). From March to May the Saharan and Arabian high pressure system weakens and moves north. Over the Red Sea the low pressure area remains and over Sudan a low pressure centre develops. During this period onshore east and south-east winds are prominent. Spring rains can occur as a result of the change in pressure cells, this small rain season is known as the *belg* season (figure 1). In May the monsoon establishes, associated with the northwards movement of the Intertropical Convergence Zone (ITCZ). Unstable, warm, moist air with eastern wind passes over the Indian Ocean and converges with the stable, continental air and provokes frontal precipitation in the eastern and southern part of Ethiopia (Westphal 1975, Seleshi and Zanke 2004). At the end of June the ITCZ is in his most northern position (16 - 12°N) initiating the main rain season from June to September, known as *kremt* (figure 1) (Cheung *et al.* 2008). *Kremt* rain is responsible for 65 to 95 % of the total annual amount of rainfall (Segele and Lamb 2005). According to Westphal (1975)

the weather during this period is dominated by the monsoon low pressure of India and Pakistan. Winds in the lower troposphere come prominently from the west and these air masses are moist and cool, as they originate from the South Atlantic and absorb vapour passing the equatorial forest, these are the main source of moisture for Ethiopia (Westphal 1975, Goebel and Odenyo 1984, Segele and Lamb 2005).

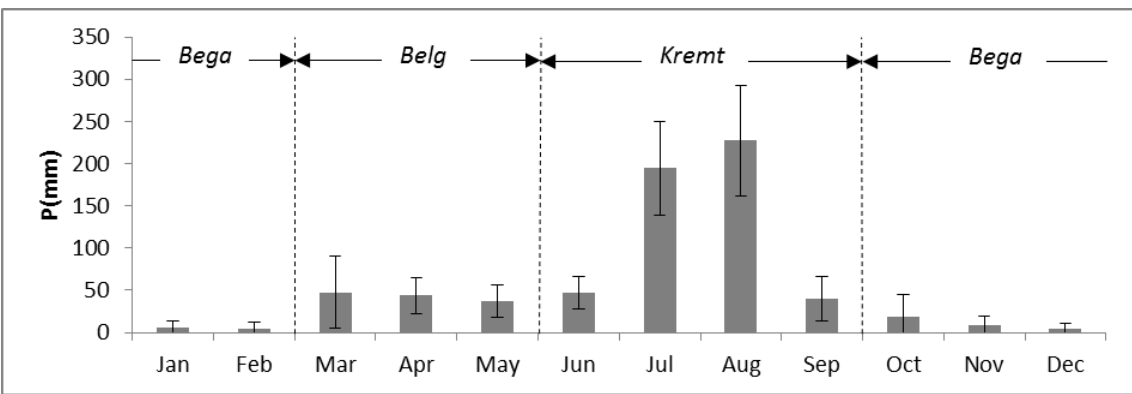


Figure 1: Rainfall averages (1996-2006) with standard deviation based upon rainfall data of the meteorological stations in the study area (without missing values). The seasonal borders are indicated by dotted lines: the *bega* (dry) season begins in October and ends on the beginning of March.

In the rain season the dominant western wind in the lower troposphere provokes more rainfall on western and southern slopes (Nyssen *et al.* 2004). As a result the North Ethiopian highlands intercept most of the monsoonal rainfall in the region, provoking a strong moisture deficit at the Rift Valley (Legesse *et al.* 2004). Tilahun (2006b) calculated the probabilities of wet and dry periods for Mekelle (regional capital of Tigray). In the period July-August the probability of a dry period of two days is very low (ca. 2%). At the same period the maximum probability for a wet day occurs, on nine August with 75%. In contrast, in the period October-February the probability of a dry period of one week is about 90%, rainfall in this period is highly unreliable. A proportion of only 2% of the rain-days is responsible for 40% of the total rainfall (Tilahun 2006b).

2. Materials and method

2.1 Study area

The Federal Democratic Republic of Ethiopia is a landlocked state of 1 104 300 km² (UN 2010) in the horn of Africa. The study area (20 800 km²) covers a north-south transect strip across the eastern part of Tigray, the most northern region of Ethiopia (figure 2). The study area is delimited to reflect the regional variability in environmental characteristics, i.e. variations in climate, topography and soil. The study area is situated on the western shoulder of the Rift Valley between 12°40' and 14°23'N and between 38°55' and 39°49'E with the towns of Adigrat in the northernmost and Maychew in the southernmost position. The elevation of the study area ranges from 1000 to 4000 m a.s.l. (at the Ferrah Amba summit) (figure 2). The relief is characterized by a stepped morphology reflecting the subhorizontal geological structure (Nyssen *et al.* 2007). Towards the east of the Tigray region, on the border with the Afar region, the altitude lowers rapidly towards the East African Rift valley. This change in topography is the water divide between the westwards drainage towards the hydrological basin of the Blue Nile and that eastward towards the basin of the East African Rift.

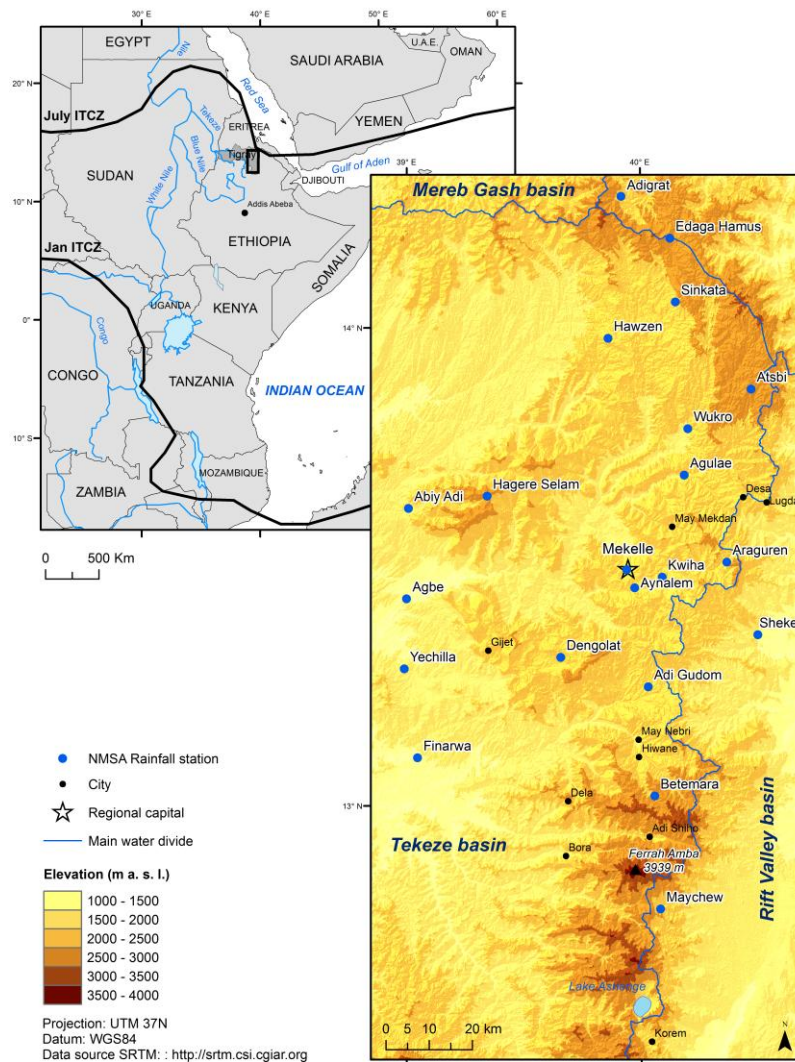


Figure 2: Location of the study area in the horn of Africa, on the western shoulder of the Rift Valley, along a north-south transect across eastern and southern Tigray. Notice the position of the ITCZ in January and July on the regional map.

2.2 Meteorological stations

The National Meteorological Agency of Ethiopia (NMA) currently has 61 meteorological stations in Tigray, classified as synoptic, principal, 3rd, and 4th class stations (NMA 2010). The stations are located in urbanised areas, leading to a lack of information within agricultural and scarcely populated areas. In this research a NMA dataset of 21 meteostations from eastern Tigray is used with rainfall data starting from the early 1960s up to 2006 (figure 3). The quality of the data strongly varies between the stations in terms of both timespan and missing records. The missing data are not

flagged as zero but are left blank or letter-coded. Four stations (Agulae, Araguren, Betemera and Finarwa) have no data for the research period (1996-2006). The remaining 17 meteorological stations are used for the calculations, this corresponds in theory with a density of 1 station every 1224 km² in the study area. But in reality the stations are unevenly distributed, they are mainly located in the north and the centre and only limited in the south of the study area.

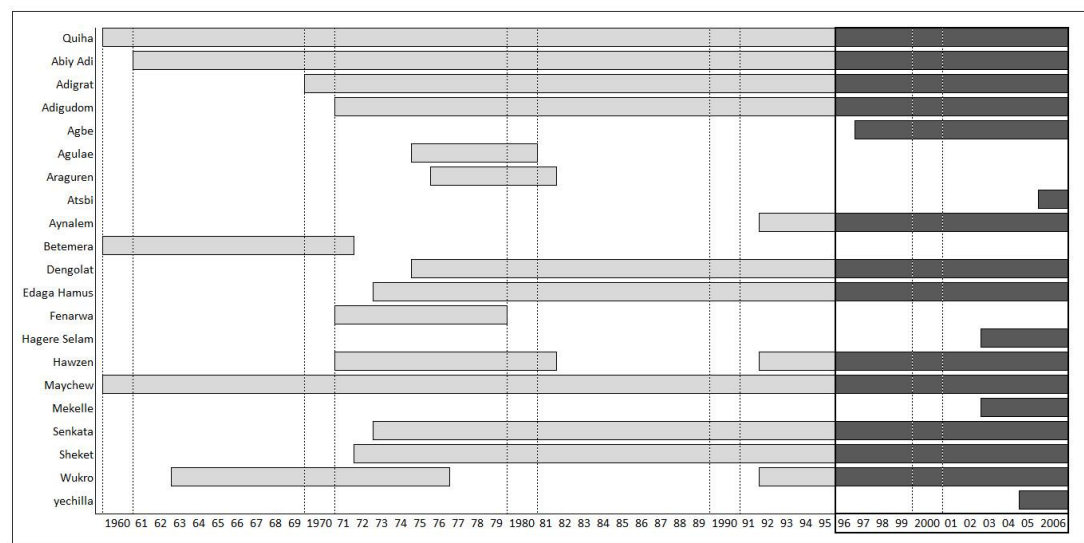


Figure 3: Rainfall measurement operation interval of the 21 NMA Meteorological Stations (1960-2006).

2.3 Spatiotemporal rainfall analysis

2.3.1 Data and pre-processing. Satellite derived Rainfall Estimates (RFEs) of North Ethiopia were accessed from the National Oceanic and Atmospheric Administration Climate Prediction Centre (NOAA-CPC) on <http://www.cpc.ncep.noaa.gov>. The decadal RFE images have a spatial resolution of 0.1° and could be downloaded over the period 1996-2006. RFEs of the period 1996-2000 are based on the algorithm developed by Herman *et al.* (1997). The 1.0 algorithm relates convective precipitation to cold cloud tops observed on Meteosat 7 infrared satellite images and orographic precipitation to warm cloud precipitation due to orographic lifting observed through the integration of surface wind direction, relative humidity and orography. The 1.0 algorithm is enhanced by incorporating rain gauge reports from approximate 1000 stations over

Africa. RFEs of the period 2001-2006 are based on the 2.0 algorithm developed by Xie and Arkin (1996). In addition to the version 1.0, RFEs version 2.0 incorporates two rainfall estimation instruments (Special Sensor Microwave/Imager and the Advanced Microwave Sounding Unit). Also in contrast to the 1.0 algorithm, warm cloud precipitation is no longer included in the algorithm.

Daily rainfall of the 17 meteorological station (MS) and decadal data of the RFE were summed to monthly data for the corresponding periods without missing MS data. Assigning MS data to specific RFEs pixels was done in ArcGIS® 9.2 by projecting the location of the rainfall station into the Albers equal area conic projection (Clarke 1866 spheroid) used for the RFEs; with as origin of latitudes 1°, central meridian 20°, first standard parallel -19°, and second standard parallel 21°(FEWS NET 2010b).

2.3.2 Validation and calibration of the Rainfall Estimates. Rainfall detection capabilities of satellite derived rainfall estimates (RFE) are less accurate over the complex topography of the semi-arid Ethiopian Highlands (Dinku *et al.* 2010). Therefore they advised to incorporate local rain gauge observations to improve the accuracy of the RFE images. In this paper a local calibration of the RFE images with meteorological stations is verified as a technique to improve the rainfall estimations and study rainfall patterns in a spatio-temporal context.

The statement by Beyene and Meissner (2010) that RFE images are less accurate in measuring rainfall in the dry season (from October to February) is also true in our study (figure 4). Consequently only the rainfall in the *belg* and *kremt* rain season, which is responsible for an average of 91% of the total yearly rainfall (1996-2006), was used to calibrate the RFE images. Rainfall in the dry season was thus neglected in the calibration model and could not be compensated by an extrapolation of the rain season. Rainfall amounts in the dry and rain season did not correlate significantly (R^2 : 0.1391, P : 0.26, 1996-2006).

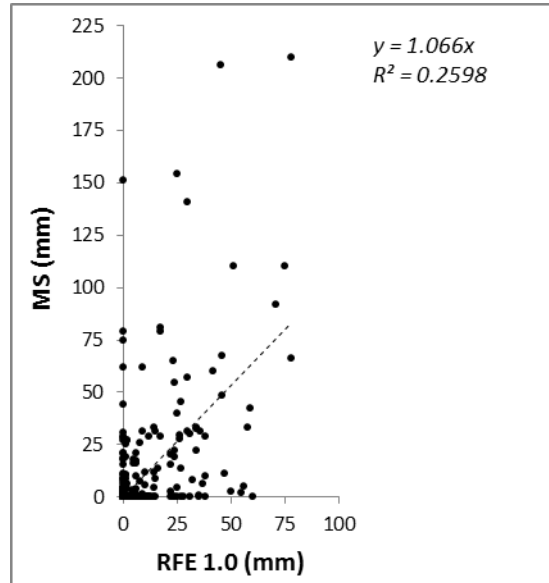


Figure 4: RFE versus MS rainfall for the dry season (1996-2000). The correlation between MS and RFE1.0 rainfall values for the dry season (October-February) is low (R^2 : 0.26).

In order to assess whether RFEs accurately estimate monthly rainfall, a linear regression analysis was performed in SPSS® 20 with MS as independent variables and RFEs (versions 1.0 and 2.0) as dependent variable (Funk and Verdin 2003, Dinku *et al.* 2007). The model was forced through the origin as this zero-zero point is the only point that fits 100% with reality. The advantage of this method is that a bias at the origin of 16mm for RFE1.0 and 12 mm for RFE2.0 is excluded from the model. The Abiy Adi station was excluded from the analysis as a large discrepancy between MS and RFEs data could be observed. Field experience learns that this was probably caused by the importance of local orographic rains as a result of the particular location of the Abiy Adi station at the foot of a steep mountain slope which rises 700 m high.

Increasing the accuracy of RFEs data for the North Ethiopian Highlands was done by calibrating the RFEs with MS data. Therefore, a stepwise multiple regression analysis through the origin with RFEs, elevation, slope and slope aspect as independent variables and MS as dependent variable was applied (Purevdorj *et al.* 1998, Weisberg 2005). Elevation, slope gradient and slope aspect were generalized from the 90m SRTM (CGIAR 2012) with the spatial analyst tools in ArcGIS® 9.2. These additional parameters were added to the regression analysis with the purpose of improving the estimation of the spatial variation of rainfall in the study area by the RFEs. The

additional parameter slope aspect can take all trigonometrical directions and is therefore fitted according to the model of Nyssen *et al.* (2005) with a sinusoidal function. The spatial variation was modelled by a non-linear multiple regression according to a stepwise model, excluding at each step the least significant explanatory variable until the best significant relation was found.

The regression equation for the calibration is thus formed by:

$$\hat{M}s = \hat{\beta} \times RFE_i + \hat{\alpha} \times S_i + \hat{\mu} \times E_i + p_1 \times (\sin(A_i - p_2)) \quad (1)$$

With:

$\hat{M}s$: estimate monthly MS rainfall (mm mth⁻¹)

RFE_i : Monthly RFEs rainfall (mm mth⁻¹)

S_i : Average slope gradient of the pixel (°)

E_i : Average elevation (m a.s.l.)

A_i : Average slope aspect (in deg. turning right from the N)

p_1 and p_2 are constants: p_1 = amplitude of the sinusoidal function and p_2 = aspect (in deg.) where average rain is expected.

The obtained calibration function is cross-validated with a robust linear model (RLM) in R® 2.14.0. The ability of the RLM function to reproduce the observed MS rainfall, in comparison to a linear model, is tested with a jackknife function.

The cross-validated calibration function was used to calibrate the monthly RFEs images over the period 1996-2006 in ArcGIS® 9.2, using a raster query. Summing up calibrated rainfall values per year gave pixel-based annual rainfall and allowed to produce an isohyet map over the period 1996-2006.

2.3.3 Explaining the spatial variability of annual rainfall. The calibrated rainfall images were used to study the explaining value of five spatial parameters (elevation, slope gradient, slope aspect, easting and northing) on the spatial distribution of rainfall for the study area (eq. 2).

$$RFE_{cal} = f(\text{elevation, slope, slope aspect, easting, northing})? \quad (2)$$

The calibrated RFE images have a resolution of 0.1°, the SRTM derived parameters (elevation, slope and slope aspect) are therefore generalised to this resolution. Subsequently a vector point grid was computed for the centre of the raster area and the pixel values were extracted for each point of all variables. The easting and northing of the pixels were calculated by adding x,y coordinates to the vector point grid. The results of these calculations in ArcGIS 9.2 are six corresponding tables. These were used as input to a multiple non-linear regression analysis to identify which variables do significantly explain the variability of annual rainfall in the study area.

3 Results

3.1 Monthly Rainfall Estimates versus Meteorological station data

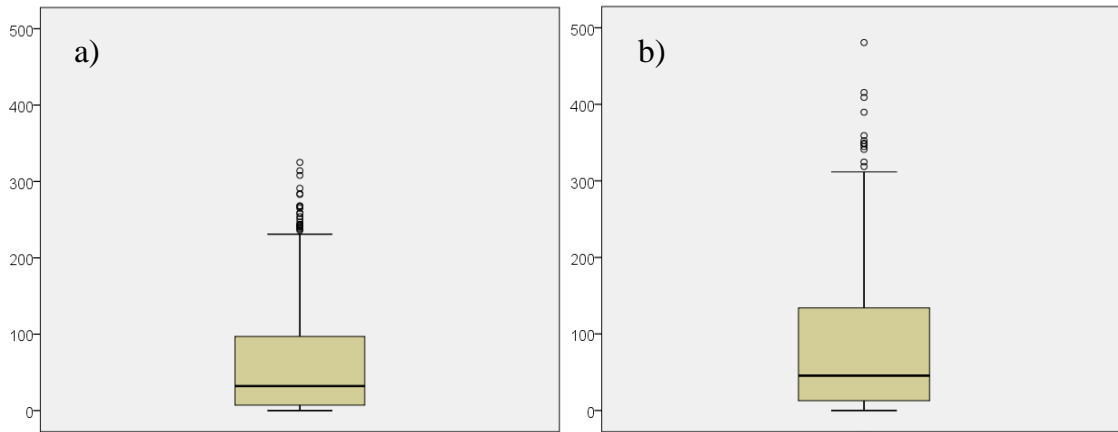
Average monthly rainfall from the sixteen MS was 85.0 mm and 79.4 mm over the periods 1996-2000 and 2001-2006 respectively (Table 1, figure 5). Over the same periods, average monthly rainfall derived from RFEs was 68.3 mm (RFE 1.0) and 59.8 mm (RFE 2.0). This means that RFEs underestimate by approximately 25% the rainfall recorded in MS. This is the result of extremely greater observations for the MS datasets (Table 1, figure 5). The Pearson's r correlation coefficient is 0.85 between MS and RFE 1.0 and 0.80 between MS and RFE 2.0. Both the skewness and kurtosis are significant at the $\alpha = 0.05$ level.

Table 1: MS and RFEs monthly rainfall (mm mth-1) over the period 1996-2006.

	1996-2000		2001-2006	
	MS	RFE 1.0	MS	RFE 2.0
Months (n)	359	359	552	552
Mean	85.0	68.3	79.4	59.8
Median	45.6	32.0	43.0	39.0
Std Deviation	96.4	81.6	85.5	60.9
Minimum	0.0	0.0	0.0	0.0
Maximum	480.7	325.0	405.3	284.0
Interquartile Range	121.3	91.0	104.6	67.0
Skewness†	1.4	1.3	1.3	1.4
Kurtosis†	1.3	0.5	1.1	1.3

† significant at $\alpha = 0.05$.

324



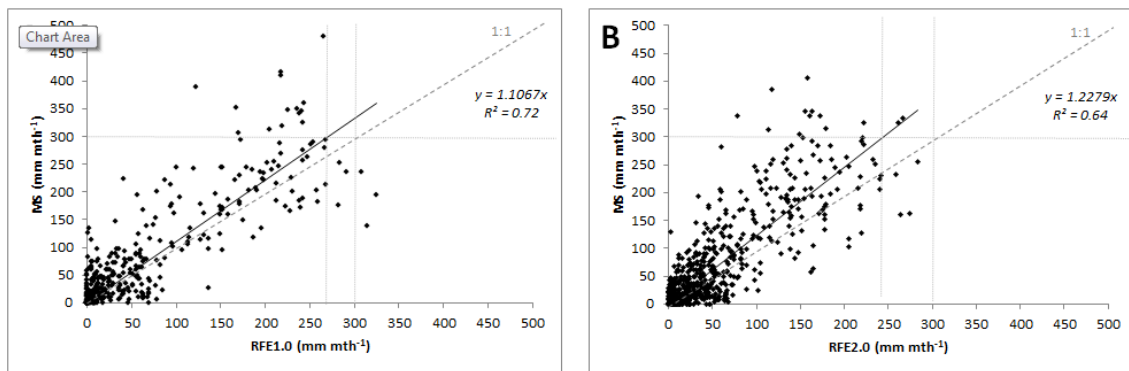
325

326

327 **Figure 5:** Boxplots of the monthly rainfall data (in mm) for the period 1996-2000 (a)
 328 RFE1.0 and (b) MS.

329

330



331

332

333 **Figure 6:** Linear regression analysis of monthly rainfall for RFEs versus MS. (a) RFEs
 334 1.0 (period 1996-2000), (b) RFEs 2.0 (period 2001-2006). Underestimation of the RFE
 335 values in comparison to 300 mm monthly rainfall in MS.

336

337 A linear regression analysis between monthly rainfall from MS and RFE 1.0 or RFE
 338 2.0 was carried out to define the estimation accuracy of the RFEs (figure 6(a) and (b)).
 339 With adjusted R^2 -values of 0.72 and 0.64 respectively ($P < 0.001$), both RFEs 1.0 and
 340 RFEs 2.0 prove to be good estimators of MS data. The validity of these models was
 341 supported by a fulfilment of the homogeneity of variance, normal distribution of the
 342 residuals, and no trends occurring when plotting the residuals against calendar years.
 343 From the line of perfect agreement (1:1 line, figure. 6(a) and (b)) it appears that RFEs
 344 generally underestimate MS rainfall, and the scatter around the trendlines indicates that
 345 the estimation of monthly rainfall by the RFE can be in gross error.

3.2 Calibrated monthly Rainfall Estimates over the period 1996-2006

Slope gradient and slope aspect have no added value as explaining factors of the spatial variation and are therefore excluded from the regression equation (Table 2). Elevation is significant but the explaining value gained by adding this variable in the regression equation is very low (R^2 increases by 0.009). The stepwise regression finally resulted in a simple linear regression through the origin (0,0) with RFE as independent variable.

The linear model (LM) is cross validated with a robust linear model (RLM). The fitted regression line of the LM and RLM function are almost identical, the RLM fitted line falls completely within the 95% confidence interval of the LM (figure 7).

The jackknife estimate of bias for the LM and RLM is respectively 0.001 and -0.012 and the jackknife estimate of the standard error is respectively 0.038 and 0.042. The difference between the jackknife estimate of the bias and standard error is insignificant. Therefore the LM is used for the calibration for the two RFE versions 1.0 and 2.0 separately.

Table 2: Coefficients and excluded variables as resulted from the non-linear multiple stepwise regression (RFE1.0, 1996-2000)

	<i>t</i> -value	<i>p</i> -value
Coefficients		
RFE1.0	31.500	0.000
Elevation	4.832	0.000
Excluded variables		
Slope gradient	-0.243	0.808
Slope aspect	-0.071	0.944

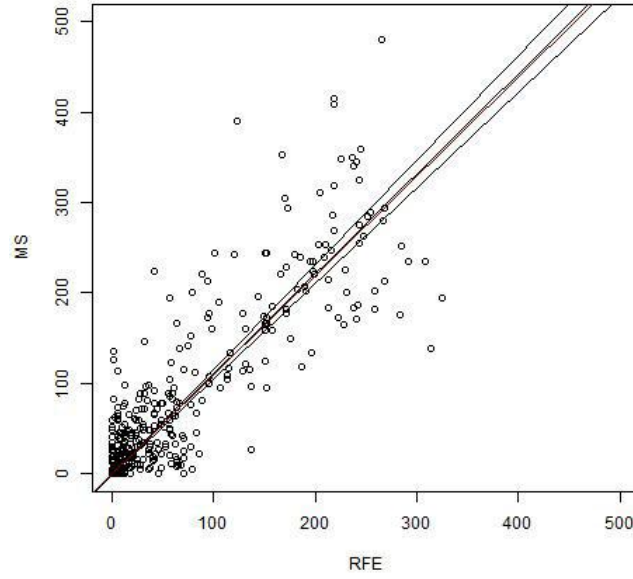


Figure 7: A comparison between the LM and RLM for RFE1.0 versus MS (1996-2000). With: in black the fitted regression line of the LM with 95% confidence interval (CI) and in red the RLM fitted regression line. Notice that the red RLM regression line lies completely within the 95% CI of the LM.

As the RFEs prove to underestimate monthly MS rainfall, a linear regression analysis with RFEs as independent variable and MS as dependent variable was performed (figure 6(a) and (b)). The linear regression equations for RFEs 1.0 and 2.0 were:

$$\hat{M}_s = 1.1067 \times RFE(1.0)_i \quad R^2: 0.72 \text{ N: } 359 \text{ P: } <0.001 \quad (3)$$

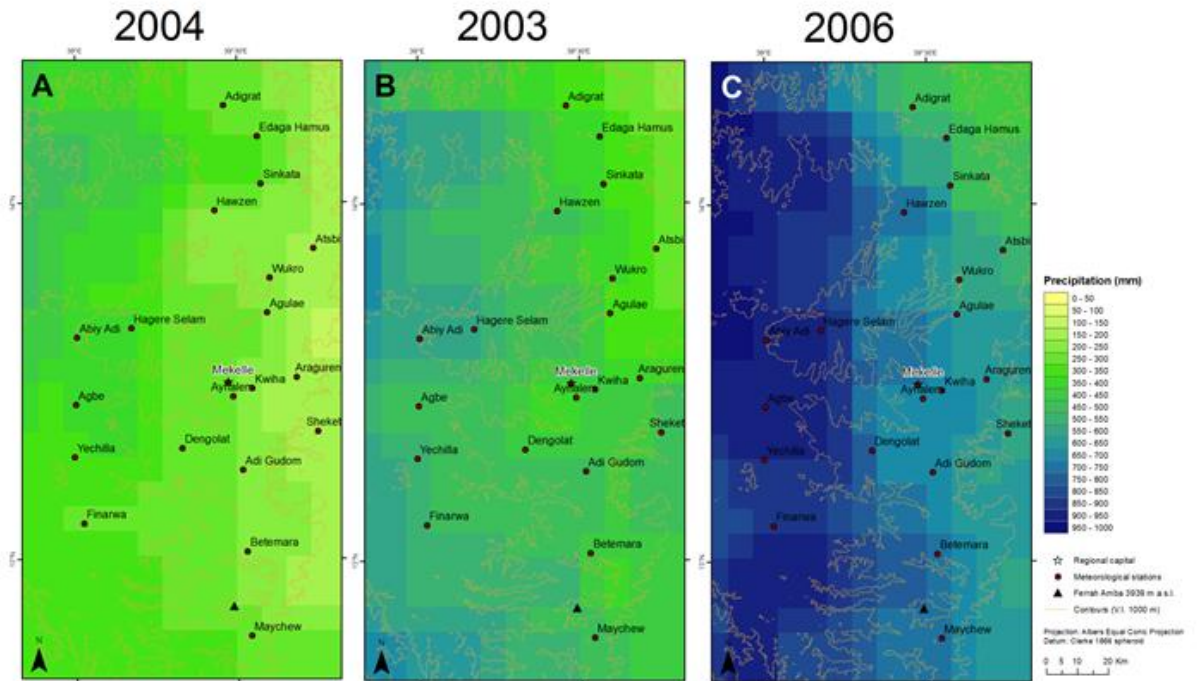
$$\hat{M}_s = 1.2279 \times RFE(2.0)_i \quad R^2: 0.64 \text{ N: } 552 \text{ P: } <0.001 \quad (4)$$

As both coefficients were significant at $P < 0.001$, calibrating the RFEs images was done by multiplying the RFEs pixel-values with 1.1067 and 1.2279 for RFEs 1.0 and RFEs 2.0. In order to validate the calibration model, a comparison of the origin RFE values and the calibrated RFE values to the MS gauge rainfall values is made. As a result of the RFE1.0 calibration, the estimation of rainfall for the study area improved by average with 8% (Table 3) in comparison to the original RFE1.0.

388 **Table 3:** Validation of calibration model for RFE1.0 (1996-2000)

	Total†			Error§		Improvement¶ of Cal RFE (%)
	Orig. RFE (mm)	Gauge Rainfall (mm)	Cal‡ RFE (mm)	Orig. RFE (%)	Cal RFE (%)	
March	897	1455.3	992.7	38.4	31.8	6.6
April	1109	1489.0	1227.3	25.5	17.6	7.9
May	1161	2051.7	1284.9	43.4	37.4	6.0
June	1516	2039.8	1677.8	25.7	17.7	7.9
July	8861	10635.5	9806.5	19.3	7.8	8.9
August	9797	10993.1	10842.3	8.6	1.4	9.5
September	1161	1838.5	1284.9	36.9	30.1	6.7
Avg. total	3500	4357.6	3873.8	28.2	20.5	7.7%

389 † Rain season total
390 ‡ Calibrated RFE: 1.1067*RFE1.0
391 § Percentage error in comparison with MS
392 ¶ Improvement of calibrated RFE in comparison with original RFE
393



394 **Figure 8:** Calibrated yearly RFEs corresponding to a typical (a) dry year (2004), (b)
395 normal year (2003) and (c) wet year (2006).
396
397
398

The monthly calibrated RFE images are summed for each year to obtain maps of the total yearly rainfall (figure 8). The calibrated RFE maps demonstrate regional and temporal yearly rainfall contrasts for the study area. Based upon these maps an isohyet map of the average yearly rainfall for the period 1996-2009 was constructed (figure 9). The isohyet map indicates that there is a general northeast-southwest gradient of increasing rainfall in the study area and a sharp east-west gradient of increasing rainfall in the north of the study area. The average annual rainfall of the southernmost MS of Maychew is only 542 mm. The average total rainfall difference between the north-eastern (320 mm) and the south-western (620 mm) part of the study area is 300 mm. However this difference fluctuates highly between the different observed years.

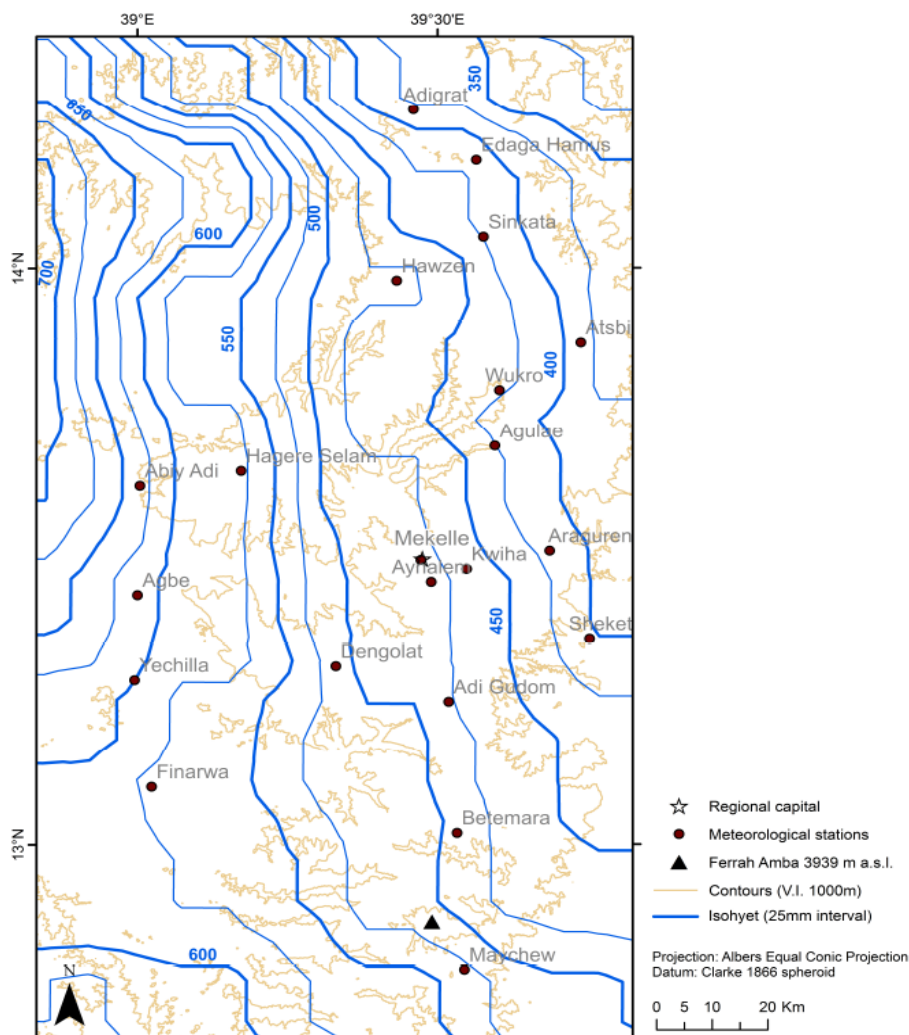


Figure 9: Isohyet map of the average rainfall (1996-2006) in the rain season (from March till September) as derived from calibrated RFE data.

3.3 Spatial variability of annual rainfall

A non-linear multiple regression is used to determine which variables are significantly explaining the variability of the annual rainfall. The regression is executed with the calibrated average of RFE1.0 as dependent variable (representing the spatial distribution of rainfall) and elevation, slope gradient, slope aspect, easting and northing as independent explaining variables. The stepwise multiple regression excludes the variables elevation, slope gradient and slope aspect, these variables are not significantly contributing in explaining the spatial distribution of the rainfall. The resulting regression equation includes easting and northing (eq. 5) and has an R^2 -value of 0.86 ($P < 0.001$). The distribution of rainfall for the study area is thus very dependent on easting and northing.

$$RFE_{cal} = 7333.581 - 0.00288029E - 0.000663432N \quad R^2: 0.86 \quad N: 325 \quad P: < 0.001 \quad (5)$$

With

E : Easting (m)

N : Northing (m)

A simple linear regression analysis between successively easting- and northing- and RFE_{cal} average (1996-2000) is given in figure 10(a) and (b). Apparent is the high explaining value of the easting (R^2 : 0.72). The east-west position is hence most important in explaining the amount of yearly rainfall for the study area. The amount of rainfall decreases eastwards. The explaining value of the northing is less strong (R^2 : 0.14), however the plotted linear trendline shows a decrease of rainfall with increasing northing. These results correspond to the trends detected from the calibrated rainfall maps (figure 8).

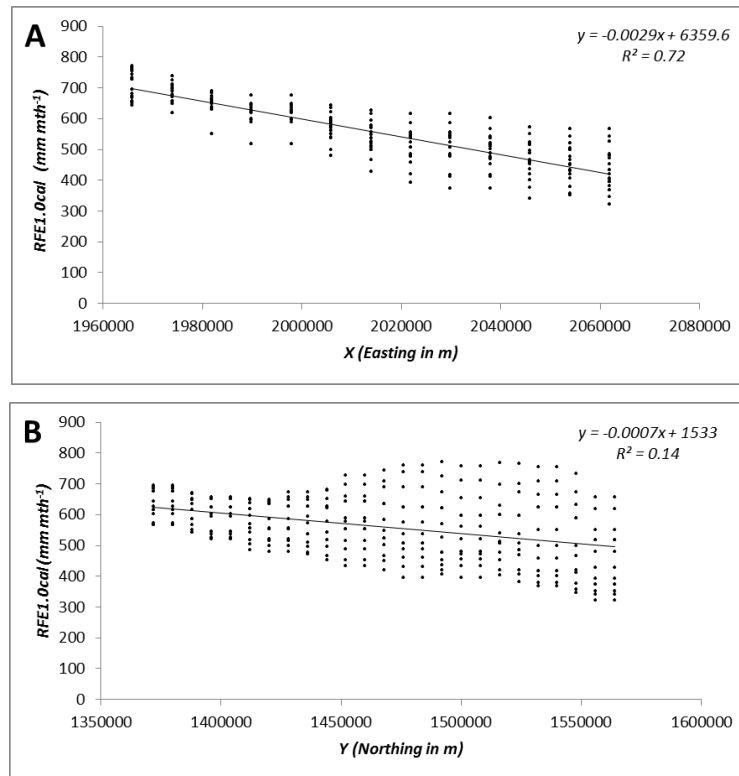


Figure 10: Linear regression analysis of longitude (a) and latitude (b) versus average annual calibrated rainfall of RFE1.0 (1996-2000) (RFE1.0cal).

4. Discussion

As indicated by this and previous studies (Dinku *et al.* 2007, Beyene and Meissner 2010), RFEs can provide fairly good insights into spatiotemporal rainfall patterns in North Ethiopia. The high correlation coefficients of 0.85 or 0.80 between monthly rainfall from MS and RFEs 1.0 or 2.0 respectively are similar to the findings of Dinku *et al.* (2007) where r -values of 0.78 and 0.75 are reported. RFE1.0 is performing 8% better than the new RFE2.0 images that seems to suffer from the exclusion of orographic warm rain processes in the RFE2.0 algorithm (Beyene and Meissner 2010). High correlations were found during the rain season (March-September) and weak correlations occurred during the dry season (October-February). To counter the weak correlation in the dry season, only the rain season rainfall from March till September is used in the calibration model. Neglecting the dry season rainfall is possible given its limited fraction of the annual rainfall (*ca.* 9%) in the North Ethiopian Highlands.

RFEs underestimate precipitation (Dinku *et al.* 2007, figure 6). According to Dinku *et al.* (2007) this is especially the result of an important underestimation of large

precipitations. The patterns of the isohyet map match patterns as described in literature (Degefu 1987, Tadesse *et al.* 2006). The calibration model succeeds to reduce the error scatter of the original RFEs, but an underestimation of rainfall remains. The study of Dinku *et al.* (2010), revealed that RFE exhibit moderate underestimations of rainfall over mountainous regions. This is also apparent in our study, especially in the southern part of the study area. The average annual rainfall of Maychew is according to the isohyet map 542 mm, but in actuality (according to the MS data) 661 mm. Rainfall in the south is thus strongly underestimated, by 119 mm for Maychew. The poor calibration in the south may also result from the very limited rainfall data available for the southern stations of Yechilla, Finarwa and Betemara. In the western MS of Agbe the annual average rainfall differs only 4mm between the RFE average (610 mm) and the actual MS average (614 mm).

The spatial variability of rainfall in the study area is mainly determined by easting and only very limited by northing. Nonetheless northing - as a result of the northwards movement of the ITCZ - is generally described as the most important explaining factor for the distribution of rainfall in Ethiopia (Goebel and Odenyo 1984, Krauer 1988). This contrast results from the location of the study area at the boundary of the Rift Valley. The general rainfall pattern is modified by the topographic boundary of the Rift Valley (Degefu 1987) and as a result the rainfall pattern of the study area is dominated by a sharp east west gradient of increasing rainfall. The scatter around the trendlines for easting increases east and for northing increases north; this indicates that rainfall variability increases in drier regions.

To further improve the reliability of the RFE calibration, additional mountain related rainfall data is necessary. This could be achieved (i) through densification of the rain-gauge network with new MS measuring rainfall in mountainous regions or (ii) by the use of rainfall proxies. An example of a rainfall proxy that is suitable in the dry tropics is the NDVI (Herrmann *et al.* 2005, Richard and Pocard 2010). Interesting perspective for future research also consists of an historical extrapolation of the spatial rainfall pattern. We would suggest a reconstruction back to the 1970s, as rainfall measurement for most of the MS starts from this period (figure 3).

5. Conclusions

The semi-arid to subhumid mountain climate with bimodal rainfall patterns of the North Ethiopian Highlands is especially vulnerable to rainfall anomalies. The rainfall estimation strength of satellite derived RFEs for the study of spatio-temporal rainfall patterns is validated to MS data with a linear regression through the origin (0,0). As a result of a weak correlation between RFE and MS rainfall data in the dry season (R^2 : 0.26), only the rain season from March till September is analysed (responsible for *ca.* 91% of the annual rainfall). The result demonstrates that the RFEs are well correlated with the MS rainfall data (85% and 80% for RFE 1.0 and 2.0 respectively). Nevertheless RFEs generally underestimate MS rainfall and scatter around the trendlines indicate that the estimation can be in gross error. To improve the RFEs for the mountainous study area, a calibration with local rain gauge data and explanatory spatial parameters was applied. The SRTM derived spatial parameters (elevation, slope gradient and slope aspect) were not significant. Consequently the calibration resulted in a linear regression through the origin (0,0) with MS as dependent variable and RFE as independent variable. Based upon the calibration model the estimations of the RFEs improved with 8%. The calibrated RFEs supported the production of annual rainfall maps for the study area and an isohyet map with the average yearly rainfall for the period 1996-2006. The maps indicate that there is a general northeast-southwest gradient of increasing rainfall in the study area and a sharp east-west gradient of increasing rainfall in the north of the study area. The explanatory value of slope, elevation, slope aspect, easting and northing for the spatial variability of annual rainfall is studied in a non-linear multiple regression with the calibrated RFE as dependent variable. Of the explanatory variables only easting and northing are significant and included in the regression analysis (R^2 : 0.86). The most important explaining variable of the spatial rainfall variability is easting (R^2 : 0.72). This results from the position of the study area at the boundary of the Rift Valley. The scatter around the individual trendlines of easting and northing demonstrate that rainfall variability increases in drier regions. Based upon the calibration model the scatter of the original RFEs can be reduced, but an overall underestimation of rainfall remains. The high underestimation of rainfall in the south of the study area is possibly the result of the more pronounced

relief. In order to make RFEs more reliable, especially in mountainous areas, additional mountain related MS rainfall data is necessary to improve the calibration of the RFE images. Another approach could be the use of NDVI data as a proxy for rainfall in the dry tropics. However calibration of RFEs for the study area has proven to be valuable in gaining improved understanding of the regional spatiotemporal rainfall patterns, which are important as input to a wide range of scientific models with direct linkage to land management strategies and scenarios.

Acknowledgements

We acknowledge the logistic assistance of Mekelle University and the VLIR-IUC program and the financial support of the Program for Flemish Travel Scholarships of the Flemish Interuniversity Council (VLIR-UOS). Thank also goes to Yohannes Gebrezehir for assistance during the fieldwork and Silke Broidioi for her help and support.

References

- BEYENE, E.G. and MEISSNER, B., 2010, Spatio-temporal analyses of correlation between NOAA satellite RFE and weather stations' rainfall record in Ethiopia. *International Journal of Applied Earth Observation and Geoinformation*, **12**, pp. 69–75.
- CGIAR, 2012, SRTM 44 10 (90 m Resolution). Available online at: <http://srtm.csi.cgiar.org> (accessed 16 April 2013).
- CHEUNG, W.H., SENAY, B. and SINGH., A., 2008, Trends and spatial distribution of annual and seasonal rainfall in Ethiopia. *International Journal of Climatology*, **28**, pp. 1723–1734.
- CONWAY, D., 2000, Some aspects of climate variability. *Ethiopian Journal of Science*, **23**, pp. 139–161.
- DANIEL, G. (Ed.), 1977, *Aspects of climate and water budget in Ethiopia*, pp. 1–71 (Addis Ababa: Addis Ababa University Press).
- DEGEFU, W., 1987, Some aspects of meteorological drought in Ethiopia. In *Drought and hunger in Africa denying famine a future*, M.H. Glantz (Ed.), pp. 23–37 (Cambridge: Cambridge University Press).
- DE MUELENAERE, S., FRANKL, A., HAILE, M., POESEN, J., DECKERS, J., MUNRO, N., VERAVERBEKE, S. and NYSSSEN, J., 2012, Historical landscape

565 photographs for calibration of Landsat land use/cover in the Northern Ethiopian
566 Highlands. *Land Degradation & Development*, in press.

567 DINKU, T., CECCATO, P., CRESSMAN, K. and CONNOR, S.J., 2010, Evaluating
568 detection skills of satellite rainfall estimates over desert locust recession
569 Regions. *Journal of Applied Meteorology and Climatology*, **49**, pp. 1322–1332.

570 DINKU, T., CECCATO, P., GROVER-KOPEC, E., LEMMA, M., CONNOR, S.J. and
571 ROPELEWSKI, C. F., 2007, Validation of satellite rainfall products over East
572 Africa's complex topography. *International Journal of Remote Sensing*, **28**, pp.
573 1503–1526.

574 FEWS NET, 2010a, Agro-Climatic Monitoring. Available online at:
575 <http://www.fews.net> (accessed 16 April 2013).

576 FEWS NET, 2010b, Africa Data Dissemination Service. Available online at:
577 <http://www.fews.net> (accessed 16 april 2013).

578 FRANKL, A., JACOB, M., HAILE, M., POESEN, J., DECKERS, J. and NYSSSEN, J.,
579 2013, Spatio-temporal variability of cropping systems and crop land cover with
580 rainfall in the Northern Ethiopian Highlands. *Soil Use and Management*,
581 submitted.

582 FRANKL, A., NYSSSEN, J., DE DAPPER, M., HAILE, M., BILLI, P., MUNRO, R.N.,
583 DECKERS, J. and POESEN, J., 2011, Linking long-term gully and river channel
584 dynamics to environmental change using repeat photography (Northern
585 Ethiopia). *Geomorphology*, 129, pp. 238–251.

586 FRANKL, A., POESEN, J., DECKERS, J., HAILE, M. and NYSSSEN, J., 2012, Gully
587 head retreat rates in the semi-arid highlands of Northern Ethiopia.
588 *Geomorphology*, 173-174, pp. 185–195.

589 FUNK, C. and VERDIN, J., 2003, Comparing satellite rainfall estimates and reanalysis
590 precipitation fields with station data for Western Kenya. *International Workshop*
591 *on Crop Monitoring for Food Security in Africa*, European Joint Research
592 Centre and UN FAO. (Nairobi).

593 GOEBEL, W. and ODENYO, V., 1984, Agroclimatic resources inventory for land-use
594 planning, Ethiopia. Technical report 2 (Rome: Food and Agriculture
595 Organization).

596 HERMAN, A., KUMAR, V.B., ARKIN, P.A. and KOUSKY, J.V., 1997, Objectively
597 determined 10 day african rainfall estimates created for famine early warning
598 systems. *International Journal of Remote Sensing*, 18, pp. 2147–2159.

599 HERRMANN, S.M., ANYAMBA, A. and TUCKER, C.J., 2005, Recent trends in
600 vegetation dynamics in the African Sahel and their relationship to climate.
601 *Global Environmental Change*, 15, pp. 394–404.

602 KRAUER, J., 1988, Rainfall, erosivity and isoerodent map of Ethiopia. Soil
603 conservation research project. Research report 15 (Bern: University of Bern with
604 the United Nations University).

605 LEGESSE, D., VALLET-COULOMB, C. and GASSE, F., 2004, Analysis of the
606 hydrological response of a tropical terminal lake, Lake Abiyata (Main Ethiopian
607 Rift Valley) to Changes in Climate and Human Activities. *Hydrological*
608 *Processes*, 18, pp. 487–504.

609 NMA, 2010, National Meteorological Agency. Available online at:
610 <http://www.ethiomet.gov.et> (accessed 16 April 2013).

611 NYSSSEN, J., MUNRO, N., HAILE, M., POESEN, J., DESCHEEMAER, K.,
612 HAREGEWEYN, N., MOEYERSONS, J. and GOVERS, G., 2007,
613 Understanding the environmental changes in Tigray□: a photographic record
614 over 30 years. Tigray Livelihood Papers, 3, pp. 1–82.

615 NYSSSEN, J., POESEN, J., MOEYERSONS, J., DECKERS, J., HAILE, M. and LANG,
616 A., 2004, Human impact on the environment in the Ethiopian and Eritrean
617 Highlands—a state of the art. *Earth-Science Reviews*, 64, pp. 273–320.

618 NYSSSEN, J., VANDENREYKEN, H., POESEN, J., MOEYERSONS, J., DECKERS,
619 J., HAILE, M., SALLES, C. and GOVERS, G., 2005, Rainfall erosivity and
620 variability in the Northern Ethiopian Highlands. *Journal of Hydrology*, 311, pp.
621 172–187.

622 PUREVDORJ, T., TATEISHI, R., ISHIYAMA, T. and HONDA, Y., 1998,
623 Relationships between percent vegetation cover and vegetation indices.
624 *International Journal of Remote Sensing*, 19, pp. 3519–3535.

625 RICHARD, Y. and POCCARD, I., 2010, A statistical study of NDVI sensitivity to
626 seasonal and interannual rainfall variations in Southern Africa. *International*
627 *Journal of Remote Sensing*, 19, pp. 2907–2920.

628 SEGELE, Z.T. and LAMB, P.J., 2005, Characterization and variability of kiremt rainy
629 season over Ethiopia. *Meteorology and Atmospheric Physics*, 89, pp. 153–180.

630 SELESHI, Y. and CAMBERLIN, P., 2005, Recent changes in dry spell and extreme
631 rainfall events in Ethiopia. *Theoretical and Applied Climatology*, 83, pp. 181–
632 191.

633 SELESHI, Y. and ZANKE, U., 2004, Recent changes in rainfall and rainy days in
634 Ethiopia. *International Journal of Climatology*, 24, pp. 973–983.

635 SENAY, G.B. and VERDIN, J., 2003, Characterization of yield reduction in Ethiopia
636 using a GIS-based crop water balance model. *Canadian Journal of Remote*
637 *Sensing*, 29, pp. 687–692.

638 SHANKO, D. and CAMBERLIN, P., 1998, The effects of the Southwest Indian Ocean
639 tropical. *International Journal of Climatology*, 18, pp. 1373 – 1388.

640 SHRESTHA, M.S., ARTAN, G.A., BAJRACHARYA, S.R. and SHARMA, R.R., 2008,
641 Using satellite-based rainfall estimates for streamflow modelling: Bagmati basin.
642 *Journal of Flood Risk Management*, 1, pp. 89–99.

643 TADESSE, M., BETRE, A., GASHAW, B., TEWODROS, T., JORDAN, C. and
644 TODD, B. (Eds.), 2006, *Atlas of the Ethiopian rural economy*, pp. 1–93 (Addis
645 Ababa: Ethiopian Development Research Institute).

646 TILAHUN, K., 2006a, The characterisation of rainfall in the arid and semi-arid regions
647 of Ethiopia. *Water SA*, 32, pp. 429–436.

648 TILAHUN, K., 2006b, Analysis of rainfall climate and evapo-transpiration in arid and
649 semi-arid regions of Ethiopia using data over the last half a century. *Journal of*
650 *Arid Environments*, 64, pp. 474–487.

651 UN, 2010, United Nations data retrieval system, country profile Ethiopia. Available
652 online at: <http://data.un.org> (accessed 16 April 2013).

653 VERDIN, J., FUNK, C., SENAY, G. and CHOULARTON, R., 2005, Climate science
654 and famine early warning. *Philosophical Transactions of the Royal Society of*
655 *Biological Sciences*, 360, pp. 2155–2168.

656 WEISBERG, S. (Ed.), 2005, *Applied linear regression*, pp. 1–352 (New York: Wiley
657 *Series in Probability and Statistics*).

658 WESTPHAL, E. (Ed.), 1975, *Agricultural systems in Ethiopia*, pp. 1– 278
659 (Wageningen: Centre for Agricultural Publishing and Documentation).

660 XIE, P. and ARKIN, P.A., 1996, Analyses of global monthly precipitation using gauge
661 observations satellite estimates, and numerical model predictions. *Journal of*
662 *Climate*, 9, pp. 840–858.

663
664
665